

## High permittivity processed SrTiO<sub>3</sub> for metamaterials applications at terahertz frequencies

Cyrielle Dupas,<sup>1,2</sup> Sophie Guillemet-Fritsch,<sup>2</sup> Pierre-Marie Geffroy,<sup>1</sup> Thierry Chartier,<sup>1</sup> Matthieu Baillergeau,<sup>3</sup> Juliette Mangeney,<sup>3</sup> Jean-Pierre Ganne,<sup>4</sup> Simon Marcellin,<sup>5</sup> Aloyse Degiron,<sup>5</sup> and Éric Akmansoy<sup>5, a)</sup>

<sup>1)</sup> *Univ Limoges, CNRS, SPCTS UMR 7315, Ctr Europeen Ceram, F-87068 Limoges, France*

<sup>2)</sup> *Univ. Paul Sabatier, CNRS, Institut Carnot, CIRIMAT, UMR 5085, F-31062 Toulouse, France*

<sup>3)</sup> *Univ Paris 06, Univ D. Diderot, CNRS, Ecole Normale Super, Lab Pierre Aigrain, UMR 8551, F-75231 Paris 05, France*

<sup>4)</sup> *Thales Research & Technology, Route Départementale 128, 91767 Palaiseau Cedex, France*

<sup>5)</sup> *Institut d'Électronique Fondamentale, Univ. Paris-Sud, Université Paris-Saclay, Orsay, F-91405; UMR8622, CNRS, Orsay, F 91405.*

(Dated: 5 October 2018)

High permittivity SrTiO<sub>3</sub> for the realization of all-dielectric metamaterials operating at terahertz frequencies was fabricated. A comparison of different processing routes evidences that Spark Plasma Sintering is the most effective sintering process to yield high density ceramic with high permittivity. We compare this sintering process with two others. The elaborated samples are characterized in the low frequency and in the terahertz frequency ranges. Their relative permittivities are compared with that a reference SrTiO<sub>3</sub> single crystal. The permittivity of the sample elaborated by Spark Plasma Sintering is as high as that the single crystal.

PACS numbers: 78.20.Ci, 77.22.Ch, 81.05.Mh, 78.67.Pt.

Keywords: Dielectrics, Ceramics, Spark Plasma Sintering, THz Time Domain Spectroscopy, Metamaterials

---

<sup>a)</sup>Electronic mail: eric.akmansoy@u-psud.fr

All-Dielectric Metamaterials (ADM) are the promising alternative to Metallic Metamaterials (MM). Metamaterials give rise to unnatural phenomena such as negative index, sub-wavelength focusing and cloaking. They are engineered materials whose unit cell generally comprises two sub-wavelength building blocks. MMs were firstly demonstrated in the microwave. However, going up to the terahertz and the optical domains has been difficult due to ohmic losses and complicated geometries. ADMs rely on the first two modes of Mie resonances of High Permittivity Resonators (HPR).<sup>1,2</sup> They do not suffer from ohmic losses and consequently benefit of low energy dissipation;<sup>2</sup> moreover, their unit cell is of simple geometry. HPRs at a few tens of microns scale are required for ADMs applications in the THz range.<sup>3</sup>

Terahertz (THz) radiation is widely defined as the electromagnetic radiation in the frequency range 0.3-3 THz. It permits to obtain physical data which are not accessible by the means of X-rays or infrared radiation. In this respect, THz radiation offer many applications in imaging, spectroscopy, chemical sensing, astronomy, security, etc. On their part, metamaterials have evolved towards the implementation of optical components.<sup>4</sup> ADMs permit to achieve a great number of fascinating phenomena (see ref. 5 for a review). They nevertheless require efficient fabrication processes to develop, namely, processes which lead to high permittivity ceramics that could be structured at the micron scale. Herein, we show that Spark Plasma Sintering makes it possible to fabricate dense high permittivity SrTiO<sub>3</sub> ceramic suitable for applications at terahertz frequencies. We compare this sintering process with two others routes: tape casting and uniaxial pressing. The structural properties of the samples were investigated by X-ray diffraction (XRD) and Scanning Electron Microscope (SEM). Then, the samples were characterized in the low frequency range and at THz frequencies by the means of Time Domain Spectroscopy (THz-TDS), and their dielectric constant was compared with that of a reference SrTiO<sub>3</sub> single crystal.

Commercial SrTiO<sub>3</sub> powder<sup>6</sup>, with a mean grain size of 0.5 $\mu$ m, is used to shape ceramic according to three different processes: Tape Casting (TC), Uniaxial Pressing (UP) and Spark Plasmas Sintering (SPS), the two former involving conventional sintering. Each fabrication process was implemented to prepare a batch of a few samples under similar conditions from the same SrTiO<sub>3</sub> powder. Their chemical composition is consequently the same.

Tape casting makes it possible to fabricate thin ceramic sheets with controlled thickness ranges from several tens to a few hundred micrometers.<sup>7</sup> A suspension consisting of the

ceramic powder dispersed in a solvent, with the help of a dispersant and containing a binder and a plasticizer, is cast onto a fixed support (Mylar<sup>®</sup> film). Once the solvent is evaporated, the thickness of the flexible green ceramic tape is around 100  $\mu\text{m}$ . Disks are cut in the tape by a laser beam to avoid stresses in the green tape. These disks are then debinded and pre-sintered at 1100°C, before undergoing conventional sintering at a temperature between 1320°C and 1350°C in air during 1h. These samples are referred to as TC hereinafter.

The SrTiO<sub>3</sub> powder is dispersed in water with addition of a binder, then granulated by spray-drying. A controlled amount of SrTiO<sub>3</sub> granules is uniaxially pressed into a steel matrix at a pressure of 200 MPa. Obtained green ceramic pellets are then debinded and pre-sintered at 1100°C, before conventional sintering at 1330°C. Then, the ceramics pellets are polished until their thickness is a few hundreds micrometers. These samples are quoted UP hereinafter.

Spark Plasma Sintering is a sintering process which relies on the heating by a pulsed electric current combined with high uniaxial pressure (around 75MPa).<sup>8,9</sup> The SrTiO<sub>3</sub> powder is set into a carbon graphite dies, through which the current is conducted. This process has several advantages because it allows fast heating and the possibility to obtain fully dense samples at comparatively lower sintering temperatures. The grain growth is greatly reduced, while the ceramic samples rapidly get very dense (usually above 98% in a 20 min cycle) ([See supplementary material](#)). The sintered SrTiO<sub>3</sub> ceramics are dark blue colored, which typifies the presence of Ti<sup>3+</sup> cations.<sup>10</sup> Indeed, during the sintering, the reducing atmosphere reduces Ti<sup>4+</sup> cations into Ti<sup>3+</sup> cations. Samples are then annealed at 850°C during a couple of hours in air so as to re-oxidize the Ti<sup>3+</sup> cations in the sample. These samples are a few hundred micrometers thick and are quoted SPS hereinafter.

The crystalline structure and phase purity were firstly observed at room temperature *via* XRD measurements using a Bruker D4 diffractometer. Then, the grain size and the morphology of the sintered ceramics were observed using SEM. Further, dielectric characterization was carried out in the kHz and the THz ranges in order to determine the dielectric constant (relative permittivity  $\epsilon'_r$  and dielectric losses  $\tan \delta$ ). On the one hand, the low frequencies dielectric measurements (100 Hz – 1 MHz) were performed by the means of an Impedance Analyzer Agilent 4294A. In the kHz range, the dielectric constant mainly depends on the chemical composition, the structure, the grain size and the density of the ceramics.<sup>11</sup> On the other hand, the terahertz dielectric properties were measured by the means of a THz-TDS

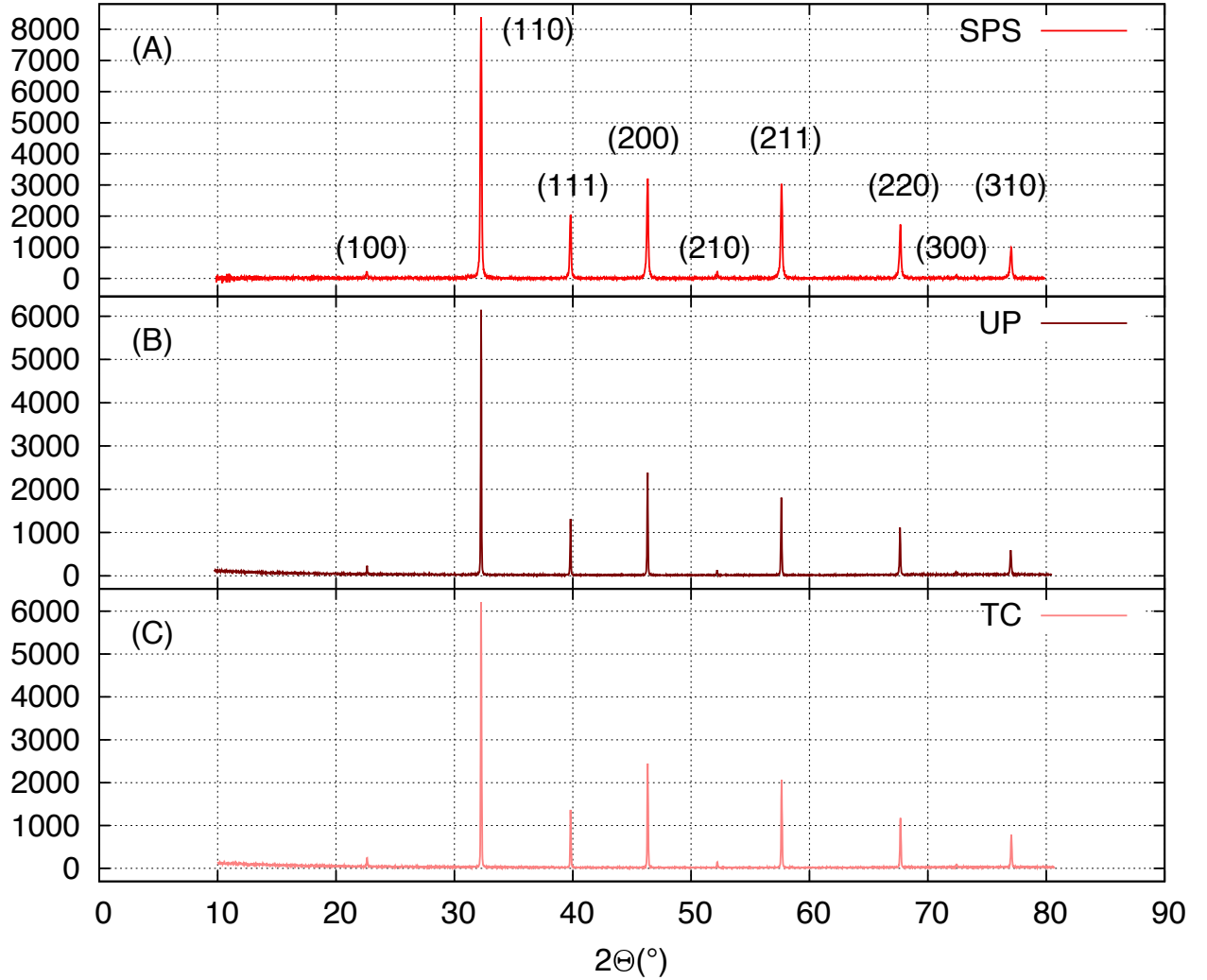


FIG. 1. : XRD patterns of sintered SrTiO<sub>3</sub> samples: (a) SPS sample, (b) UP sample, (c) TC sample. The samples are in the same crystalline phase (JCPDS 01-070-8508).

set up.<sup>12</sup> The TDS setup is based on a Ti:Sa laser (pulse duration 15 fs, central wavelength 800 nm) that is split into a pump and a probe beams. The former is converted into THz radiation (pulse duration in the picosecond range) using a photoconducting antenna patterned on a low-temperature GaAs substrate. It is then focused on the sample and the transmitted signal is measured *via* electro-optic detection. To this aim, it is combined with the probe beam which samples the THz signal thanks to a delay line. Using this technique, the temporal shape of the THz signal and its delay with respect to a reference measurement, made without sample, are obtained. The data are subsequently Fourier transformed to obtain a transmission spectrum in the frequency domain. Finally, the values of the optical index is

derived from these measurements by inverting the Fresnel equations that describe the THz transmission through the samples.<sup>13,14</sup>

XRD analyses were performed on the batches of sintered ceramics (Fig. 1). Whatever the shaping process, all the samples are in the same crystalline phase, namely, the cubic perovskite structure of SrTiO<sub>3</sub>. Then, the relative density  $d$  of the samples was measured by Archimed's method (Table I).<sup>15</sup> The relative density of the TC samples is low:  $d \approx 70\%$ , whereas that of the UP samples is improved, ranging from  $d = 90\%$  to  $95\%$ . At last, the SPS samples exhibit the highest density:  $d \geq 99\%$ . In addition, whatever the shaping process, the mean grain size of the samples, observed by SEM, is about  $0.5 \mu\text{m}$  (Fig. 2). Consequently, as the chemical composition, the structure and the grain size are identical whatever the implemented process, only the density of the samples may affect their dielectric constant.

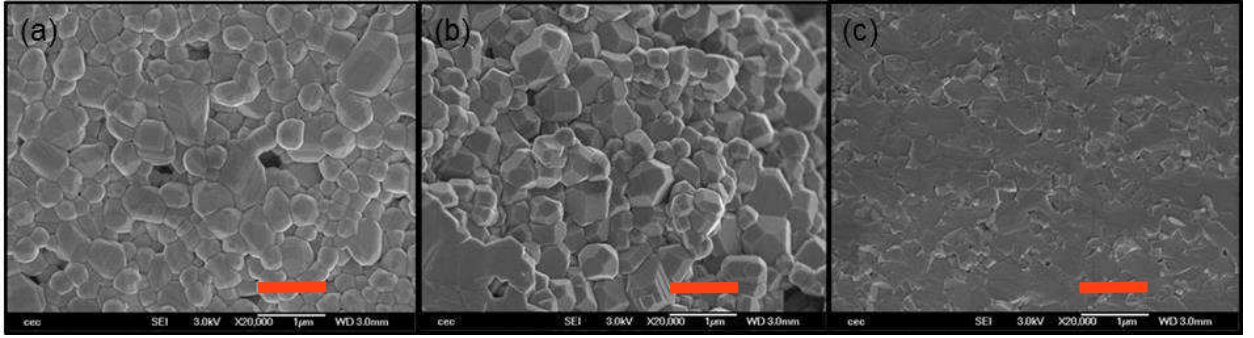


FIG. 2. SEM images of sintered SrTiO<sub>3</sub> samples: (a) TC sample, (b) UP sample, (c) SPS sample. Scale =  $1 \mu\text{m}$  (orange dash). Porosity can be noticed in the TC sample.

The dielectric constants were firstly compared at 1 kHz (Table I). The relative permittivity of the TC samples slightly increases with the density  $d$  from  $\epsilon'_r = 236$  to  $253$ , while the dielectric losses remain around  $\tan \delta = 0.02$ . The relative permittivity of the UP increases from  $\epsilon'_r = 280$  to  $289$ , as the density increases from  $d = 90\%$  to  $95\%$ , while the dielectric losses significantly decrease from  $\tan \delta = 0.02$  to  $0.002$ . At last, the SPS samples exhibit the highest relative permittivity:  $\epsilon'_r > 320$ . This process therefore yields very dense samples ( $d \geq 99\%$ ), whose relative permittivity at 1 kHz is the highest ( $\epsilon'_r > 320$ ) of the three batches and whose dielectric losses are very low ( $\tan \delta \leq 0.005$ ).

We further carried out the dielectric characterization in the terahertz range. A SrTiO<sub>3</sub> single crystal<sup>16</sup> serves as a reference in the THz set-up. Its dielectric constant was measured in the 0.2–0.9 THz range: the relative permittivity is  $\epsilon'_r \simeq 345$ , while the dielectric losses

TABLE I. Density and dielectric constant at 1 kHz of SrTiO<sub>3</sub> samples according to the shaping process.

<i>Shaping process</i>	<i>Sample</i>	<i>Density d</i>	$\epsilon'_r/\tan \delta$ (1 kHz)
Tape casting & conventional sintering	TC-STO-6a	67%	236/0.022
	TC-STO-PM1	71%	253/0.02
	TC-STO-1	73%	—
Uniaxial pressing & conventional sintering	UP-STO-2	91%	280/0.02
	UP-STO-4	93%	280/0.015
	UP-STO-7	95%	289/0.002
Spark Plasma Sintering	SPS-035	$\geq 99\%$	338/0.002
	SPS-036	$\geq 99\%$	360/0.005
	SPS-100	$\geq 99\%$	327/0.002
	SPS-101	$\geq 99\%$	—

practically linearly increase from  $\tan \delta = 0.02$  to 0.08 (Fig. 3). These results are in good agreement with those of ref. 17. The dielectric constant of three differently processed samples are reported in Fig. 3 as well. The TC samples show low relative permittivity ( $\epsilon_r \simeq 117$ ) and high losses ( $\tan \delta > 0.14$ ). Due to the porosity, the measured sample is a composite medium made of SrTiO<sub>3</sub> and air, and its dielectric constant is an effective quantity  $\epsilon_{eff}$  which is commonly described by the Bruggeman effective medium approximation (EMA).<sup>18</sup> Porosity consequently lowers the relative permittivity  $\epsilon'_r$  and increases the losses  $\tan \delta$ . The UP sample exhibits improved relative permittivity ( $\epsilon'_r \simeq 290$ ) and losses which also increase with the frequency in accordance with the PH model. The higher density similarly leads to increased relative permittivity  $\epsilon'_r$  in the terahertz range. Indeed, the relative permittivity of the SPS sample is actually close to that of the single crystal, i.e.  $\epsilon'_r \simeq 340$ , while the dielectric losses, increasing from  $\tan \delta \simeq 0.055$  at 0.3 THz to  $\simeq 0.012$  at 0.9 THz, are about 1.3 times those of the single crystal. We ascribe this point to the coexistence of Ti<sup>4+</sup> and Ti<sup>3+</sup> cations in the sample<sup>19</sup> and to grain boundaries which do not exist in single crystals. Defects and grain boundaries may increase the mobility of atomic species and then losses. Fig. 3 clearly demonstrates that the higher the density, the higher the relative permittivity  $\epsilon'_r$  and the lower the dielectric losses  $\tan \delta$ .

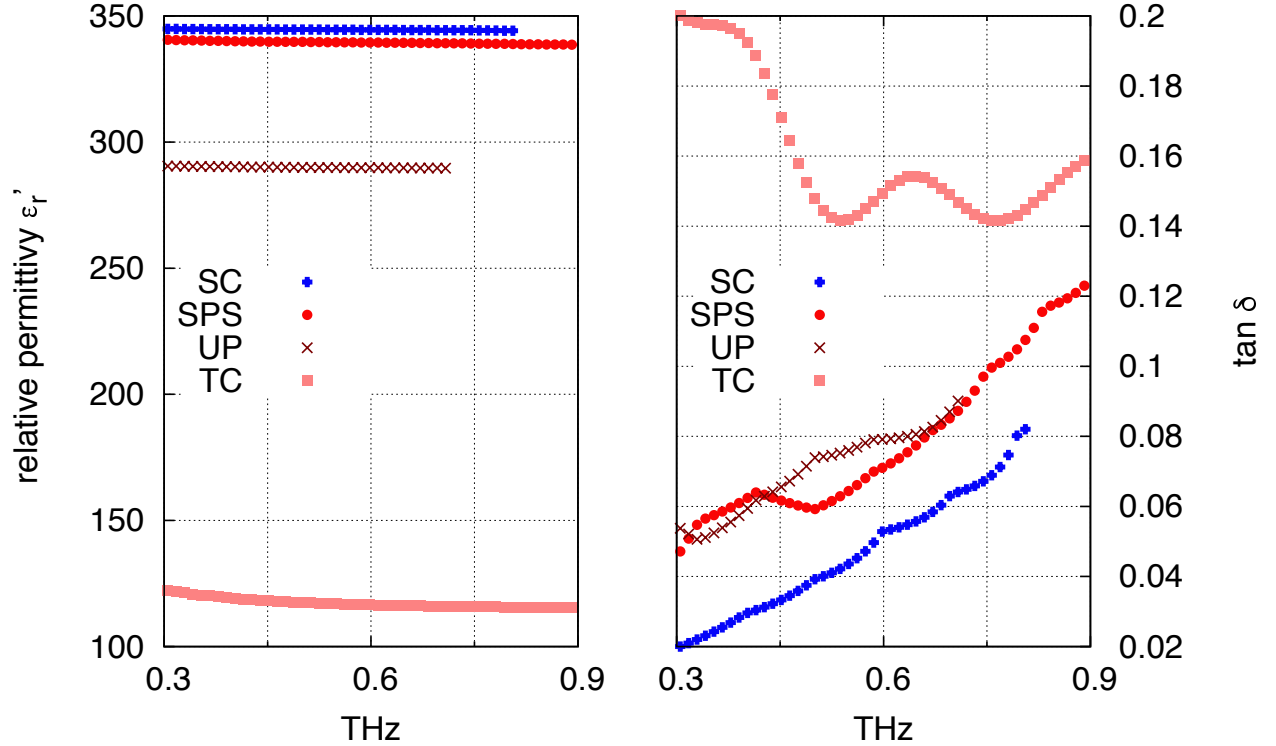


FIG. 3. : Permittivity  $\epsilon'_r$  and dielectric losses  $\tan \delta$  in the terahertz range measured by THz-TDS of different processed SrTiO<sub>3</sub> samples.

The dielectric response  $\epsilon_r(\omega)$  of SrTiO<sub>3</sub> is dispersive, because of the lattice vibrations, namely, the optical phonons.<sup>20,21</sup> Their frequency is in the THz range, and we are concerned by the Transverse Optical phonon of lowest frequency (TO1). The TO1 phonon frequency of SrTiO<sub>3</sub> is 2.70THz.<sup>20,21</sup> The dielectric function  $\epsilon_r(\omega)$  is described by the PH model (see eq.2 in ref.18), which is reported in fig.4. Losses (imaginary part of  $\epsilon_r(\omega) = \epsilon''_r$ ) resulting from the TO1 phonon greatly increase at terahertz frequencies. Measurements in both frequency ranges are also reported in fig.4 and are in good agreement with the PH model.

Fully dense SrTiO<sub>3</sub> material sintered by SPS, with a permittivity as high as that of the single crystal, is suitable for ADM applications at THz frequencies. The dielectric constant is in good agreement with the PH model. SPS is the effective process required by ADMs to develop.

This work was supported by the Agence Nationale de la Recherche under the TraMtaDiel convention (grant ANR-12-BS03-0009). É.A. thanks Fabrice Rossignol for his help.

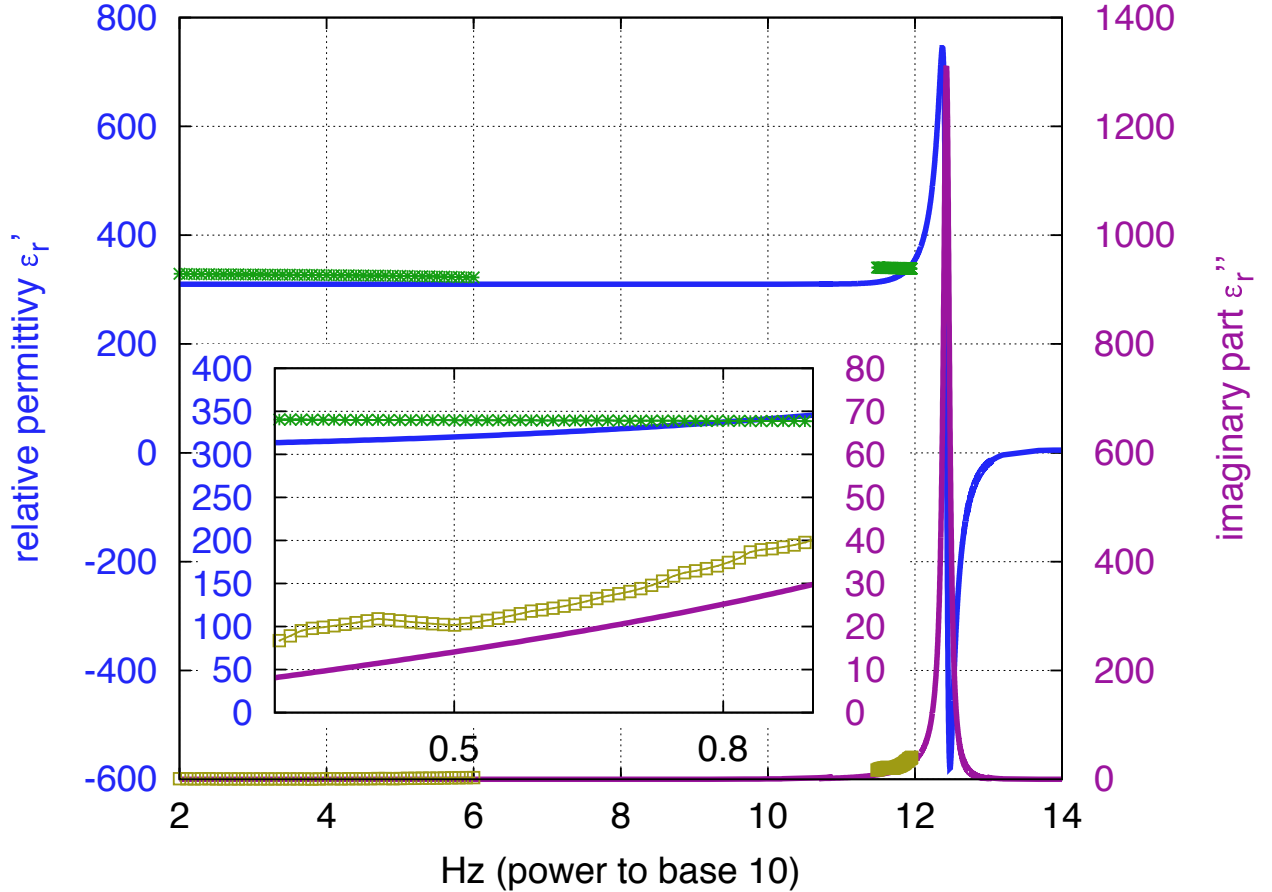


FIG. 4. : PH model of the dielectric response of SrTiO<sub>3</sub> between 10<sup>2</sup> and 10<sup>14</sup> Hz:  $\epsilon_r(\omega) = \epsilon'_r + i \epsilon''_r$  ( $\epsilon''_r = \tan \delta \times \epsilon'_r$ ) and measurements in the low frequency (100Hz–1MHz) and the THz frequency ranges of SPS sample (green and yellow-green points). Inset : zoom between 0.3 and 0.9 THz

## REFERENCES

- <sup>1</sup>A. Ahmadi and H. Mosallaei, “Physical configuration and performance modeling of all-dielectric metamaterials,” *Phys. Rev. B* **77**, 045104 (2008).
- <sup>2</sup>B.-I. Popa and S. A. Cummer, “Compact dielectric particles as a building block for low-loss magnetic metamaterials,” *Phys. Rev. Lett.* **100**, 207401 (2008).
- <sup>3</sup>F. Gauffillet, S. Marcellin, and E. Akmansoy, “Dielectric metamaterial-based gradient index lens in the terahertz frequency range,” *IEEE Journal of Selected Topics in Quantum Electronics* **PP**, 1–1 (2016).
- <sup>4</sup>N. I. Zheludev and Y. S. Kivshar, “From metamaterials to metadevices,” *Nat Mater* **11**, 917–924 (2012).

- <sup>5</sup>S. Jahani and Z. Jacob, “All-dielectric metamaterials,” *Nat Nano* **11**, 23–36 (2016).
- <sup>6</sup>Marion Technologies <http://www.mariontechnologies.com/nanomateriaux/>.
- <sup>7</sup>P. Boch and T. Chartier, “Ceramic processing techniques : the case of tape-casting,” *Ceram. For. Int.* **4**, 55 (1989).
- <sup>8</sup>M. Omori, “Sintering, consolidation, reaction and crystal growth by the spark plasma system (sps),” *Materials Science and Engineering: A* **287**, 183 – 188 (2000).
- <sup>9</sup>M. Nygren and Z. Shen, “On the preparation of bio-, nano- and structural ceramics and composites by spark plasma sintering,” *Solid State Sciences* **5**, 125 – 131 (2003).
- <sup>10</sup>C. Voisin, S. Guillemet-Fritsch, P. Dufour, C. Tenailleau, H. Han, and J. C. Nino, “Influence of oxygen substoichiometry on the dielectric properties of BaTiO<sub>3</sub> nanoceramics obtained by spark plasma sintering,” *International Journal of Applied Ceramic Technology* **10**, E122–E133 (2013).
- <sup>11</sup>B. Li, X. Wang, L. Li, H. Zhou, X. Liu, X. Han, Y. Zhang, X. Qi, and X. Deng, “Dielectric properties of fine-grained BaTiO<sub>3</sub> prepared by spark-plasma-sintering,” *Materials Chemistry and Physics* **83**, 23 – 28 (2004).
- <sup>12</sup>M. Baillergeau, K. Maussang, T. Nirrengarten, J. Palomo, L. H. Li, E. H. Linfield, A. G. Davies, S. Dhillon, J. Tignon, and J. Mangeney, “Diffraction-limited ultrabroadband terahertz spectroscopy,” *Scientific Reports* **6**, 24811 EP – (2016).
- <sup>13</sup>L. Duvillaret, F. Garet, and J. L. Coutaz, “A reliable method for extraction of material parameters in terahertz time-domain spectroscopy,” *IEEE Journal of Selected Topics in Quantum Electronics* **2**, 739–746 (1996).
- <sup>14</sup>K. Berdel, J. G. Rivas, P. H. Bolivar, P. de Maagt, and H. Kurz, “Temperature dependence of the permittivity and loss tangent of high-permittivity materials at terahertz frequencies,” *IEEE Transactions on Microwave Theory and Techniques* **53**, 1266–1271 (2005).
- <sup>15</sup>H. Sasaki, E. Tokizaki, K. Terashima, and S. Kimura, “Density variation of molten silicon measured by an improved archimedian method,” *Japanese Journal of Applied Physics* **33**, 3803 (1994).
- <sup>16</sup>Verneuil growth and cubic perovskite structure – CrysTec GmbH <http://www.crystec.de/>.
- <sup>17</sup>N. Matsumoto, T. Fujii, K. Kageyama, H. Takagi, T. Nagashima, and M. Hangyo, “Measurement of the soft-mode dispersion in SrTiO<sub>3</sub> by terahertz time-domain spectroscopic ellipsometry,” *Japanese Journal of Applied Physics* **48**, 09KC11 (2009).

<sup>18</sup>J. Han, F. Wan, Z. Zhu, and W. Zhang, “Dielectric response of soft mode in ferroelectric SrTiO<sub>3</sub>,” *Applied Physics Letters* **90**, 031104 (2007), <http://dx.doi.org/10.1063/1.2431448>.

<sup>19</sup>A longer annealing after sintering could have lowered the numbers of Ti<sup>3+</sup> cations.

<sup>20</sup>W. G. Spitzer, R. C. Miller, D. A. Kleinman, and L. E. Howarth, “Far infrared dielectric dispersion in BaTiO<sub>3</sub>, SrTiO<sub>3</sub>, and TiO<sub>2</sub>,” *Phys. Rev.* **126**, 1710–1721 (1962).

<sup>21</sup>A. S. Barker, “Temperature dependence of the transverse and longitudinal optic mode frequencies and charges in SrTiO<sub>3</sub> and BaTiO<sub>3</sub>,” *Phys. Rev.* **145**, 391–399 (1966).

## High permittivity processed SrTiO<sub>3</sub> for metamaterials applications at terahertz frequencies

### Supporting Data & Supplementary Material

Cyrielle Dupas,<sup>1,2</sup> Sophie Guillemet-Fritsch,<sup>2</sup> Pierre-Marie Geffroy,<sup>1</sup> Thierry Chartier,<sup>1</sup> Matthieu Baillergeau,<sup>3</sup> Juliette Mangeney,<sup>3</sup> Jean-Pierre Ganne,<sup>4</sup> Simon Marcellin,<sup>5</sup> Aloyse Degiron,<sup>5</sup> and Éric Akmansoy<sup>5, a)</sup>

<sup>1)</sup> *Univ Limoges, CNRS, SPCTS UMR 7315, Ctr Europeen Ceram, F-87068 Limoges, France*

<sup>2)</sup> *Univ. Paul Sabatier, CNRS, Institut Carnot, CIRIMAT, UMR 5085, F-31062 Toulouse, France*

<sup>3)</sup> *Univ Paris 06, Univ D. Diderot, CNRS, Ecole Normale Super, Lab Pierre Aigrain, UMR 8551, F-75231 Paris 05, France*

<sup>4)</sup> *Thales Research & Technology, Route Départementale 128, 91767 Palaiseau Cedex, France*

<sup>5)</sup> *Institut d'Électronique Fondamentale, Univ. Paris-Sud, Université Paris-Saclay, Orsay, F-91405; UMR8622, CNRS, Orsay, F 91405.*

(Dated: 5 October 2018)

PACS numbers: 78.20.Ci, 77.22.Ch, 81.05.Mh, 78.67.Pt.

Keywords: Dielectrics, Ceramics, Spark Plasma Sintering, THz Time Domain Spectroscopy, Metamaterials

---

<sup>a)</sup>Electronic mail: eric.akmansoy@u-psud.fr

## I. SUPPORTING DATA & SUPPLEMENTARY MATERIAL

### A. Tape casting

The suspension consists of the ceramic powder: - 29 %vol, solvent: Ethanol – 42 %vol, dispersant 1 %vol, binder: Methyl methacrylate – 13 %vol and softening agent: Dibutyl phtalate – 15 %vol

### B. Spark Plasma Sintering (SPS)

To densify the SrTiO<sub>3</sub> nanopowders, SPS was carried out using a Dr. Sinter 2080 device from Sumitomo Coal Mining (Fuji Electronic Industrial, Saitama, Japan). Briefly, 0.5 g of powder was loaded in an 8-mm-inner-diameter graphite die. A sheet of graphitic paper was placed between the punch and the powder as well as between the die and the powder for easy removal of the pellet after sintering. Powders were sintered in vacuum (residual cell pressure  $< 10 Pa$ ) at 1150°C during 3 minutes, with a pressure of 75 MPa.. An optical pyrometer focused on a small hole at the surface of the die was used to measure and monitor the temperature. The as-sintered pellets presented a thin carbon layer due to graphite contamination from the graphite sheets. This layer was removed by polishing the surface.. Samples appeared dark blue, consistent with the presence of Ti<sup>3+</sup> caused by the reducing atmosphere used during SPS (low vacuum). 21 SPS pellets were annealed in air atmosphere at 850°C in an attempt to restore the oxygen stoichiometry.

#### References

E124 International Journal of Applied Ceramic Technology — Voisin, *et al.* Vol. 10, No. S1, 2013

### C. X-Ray Diffraction (XRD)

The crystalline structure was investigated by X-ray diffraction analysis using a D4 Endeavor X-ray diffractometer (CuK $\alpha$  = 0.154056 nm and CuK $\beta$  = 0.154044 nm, operating voltage 40 kV and current 40 mA). The grain size and morphology of the powders and the microstructure of the sintered ceramics were observed with a scanning electron microscope (SEM, JEOL JSM 6400).

D. Terahertz Time Domain Spectroscopy (THz – TDS)

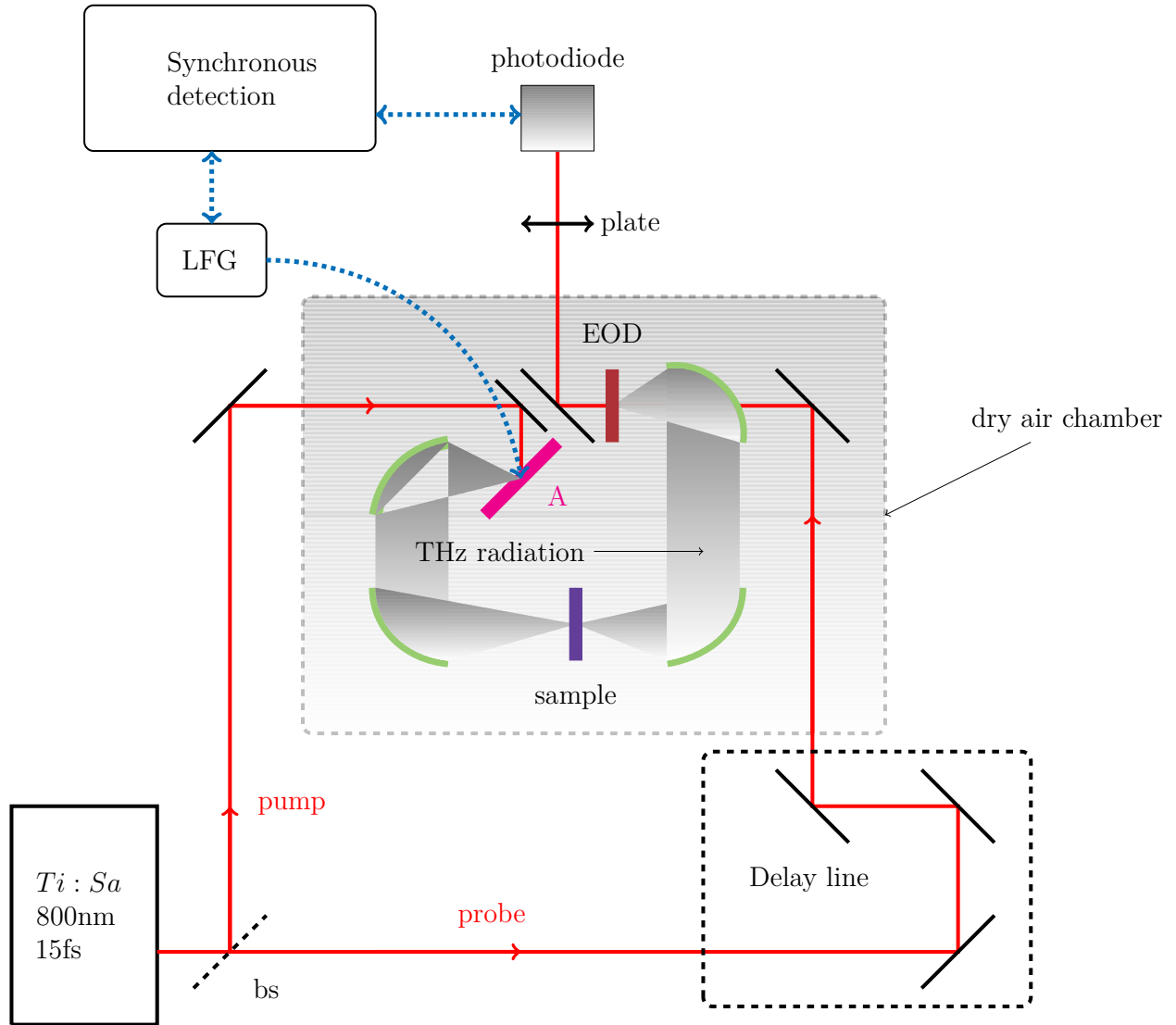


FIG. 1. Schematic layout of the THz-Time Domain Spectroscopy set-up : A stands for photoconductive antenna; EOD for Electro-optic Detection; LFG for Low Frequency Generator; bs for beam-splitter. The shaded area denotes where the THz radiation lies.